Non-linear and adaptive control of a refrigeration system

Rasmussen, Henrik; Larsen, Lars F. S.

Published in:
IET Control Theory & Applications

DOI (link to publication from Publisher):
10.1049/iet-cta.2009.0156

Publication date:
2011

Document Version
Early version, also known as pre-print

Nonlinear and adaptive control of a refrigeration system

Henrik Rasmussen[a], Lars F. S. Larsen[b]

[a]*Department of Electronic Systems, Aalborg University, Denmark (hr@es.aau.dk)*
[b]*Danfoss A/S, Nordborg, Denmark (Lars.Larsen@Danfoss.com)*

Abstract

In a refrigeration process heat is absorbed in an evaporator by evaporating a flow of liquid refrigerant at low pressure and temperature. Controlling the evaporator inlet valve and the compressor in such a way that a high degree of liquid filling in the evaporator is obtained at all compressor capacities ensures a high energy efficiency. The level of liquid filling is indirectly measured by the superheat. Introduction of variable speed compressors and electronic expansion valves enables the use of more sophisticated control algorithms, giving a higher degree of performance and just as important are capable of adapting to variety of systems. This paper proposes a novel method for superheat and capacity control of refrigeration systems; namely by controlling the superheat by the compressor speed and capacity by the refrigerant flow. A new low order nonlinear model of the evaporator is developed and used in a backstepping design of a nonlinear adaptive controller. The stability of the proposed method is validated theoretically by Lyapunov analysis and experimental results show the performance of the system for a wide range of operating points. The method is compared to a conventional method based on a thermostatic superheat controller.

NOMENCLATURE

p	time derivative operator d/dt
L_e	length of the evaporator
l_e	length of the evaporator two phase section
$\dot{m}_e$	refrigerant mass flow rate
h_i	specific enthalpy, inlet evaporator
h_g	specific enthalpy, end of two phase section evaporator
h_o	specific enthalpy, outlet evaporator
h_{lg}	specific evaporation energy, refrigerant
T_e	refrigerant boiling temperature
P_e	refrigerant pressure, evaporator
f_{comp}	compressor speed
f_{min}	minimum compressor speed $f_{min} = 35Hz$
T_{SH}	superheat, evaporator
T_w	temperature of water into the evaporator
$\dot{m}_w$	mass flow of water
c_w	specific heat capacity of water
$c_{p,e}$	constant pressure specific heat of refrigerant
α_1	heat transfer coefficient refrigerant-water
B	width of evaporator
H	hight of evaporator
γ_e	void fraction

1. Introduction

Refrigeration systems are widely used as well in applications for private consumers as for the industry. Despite differences in size and number of components, the main construction with an expansion valve, an evaporator, a compressor and a condenser, remains to a considerable extent the same. Large parts of the same technological challenges are therefore encountered in both markets. In this paper we focus on a small water chiller, however the generality of the results applies to a larger family of so-called 1:1 systems, i.e. system with 1 evaporator and 1 compressor. Refrigeration and air conditioning, accounts for a huge part of the total global energy consumption, hence improving energy efficiency in these system can potentially lead to a tremendous reductions in the energy consumption. Optimizing the set-points of these systems has been proved to enable a substantial reduction in the power consumption as shown in [1]. In [2] a method for on-line optimization of the set-points to minimize power consumption is presented. In a refrigeration system one of the key variables to control, which greatly affects the efficiency of the system, is the superheat. The superheat is used as an indirect measure of the liquid fraction of refrigerant in the evaporator. To utilize the potential of the evaporator to its maximum, the superheat should be kept as low as possible, i.e. the liquid fraction should be as high as possible. The superheat is traditionally controlled by adjusting the opening degree of the expansion valve. This is a common control strategy and examples can be found in e.g. [3] and [4]. Mechanical thermostatic expansions valves (TXV) is currently the preferred choice as expansion device in numerous applications. TXV's are relatively inexpensive and deliver a good control performance if designed and sized correctly. Designing and sizing TXV's is not always straight forward and once installed, the possibility of adjusting it to fit the specific application, is rather limited. Furthermore regarding production it requires many differentiated versions to fit the various applications. These shortcomings have opened for the introduction of electronic valves, which enable the use of more sophisticated control algorithms that potentially can overcome these difficulties. Controlling the superheat using standard SISO PID control, however often leads to poor performance, caused by mainly two major challenges. Firstly; the superheat is strongly coupled with the operation of the compressor. Neglecting this often leads to instability or the so-called hunting phenomena, see [5]. Secondly; the fact that the superheat acts highly nonlinear, depending on the point of operation and the evaporator design, limits the obtainable performance with standard PID controllers.

Previous works by [6] and [7] have proved that gain scheduling is a way to handle gain variations. In [8] a new promising model based control designs that take the cross couplings between the (uncontrollable) compressor and the valve into account, has started to emerge. By the introduction of variable speed compressors, an additional control variable that can be actively used has been introduced. [9] presents a new non-linear control strategy where the compressor is controlling the superheat and the valve is controlling cooling capacity. Recently this result has been improved in [10], where a new non-linear control strategy using a backstepping method based on Lyapunov theory is applied for improving stability. These techniques definitely show an improved performance However they rely on a detail knowledge of specific system parameters, which are typically not available for a large part of the applications. Furthermore the focus on limiting the use of refrigerants (greenhouse gases) and increasing prizes on raw material have driven the introduction of new evaporator designs on a market, that is characterized by a low internal volume. Examples of such evaporators are micro channel and plate heat exchangers. Due to the low internal volume and thereby faster dynamics, these evaporators add to the above mentioned control challenges.
To accommodate the control challenges introduced by these evaporator types and the requirements for adaptation this paper further develops the result presented in [10] with an adaptation routine to estimate unknown system specific parameters.
With the new controller it is possible to make continuous control down to zero cooling power.
Because the backstepping design is based on Lyapunov stability, the stability of the control and the adaptation can be guaranteed. By using this approach a nearly perfect decoupling between capacity and superheat temperature, for reasonable choice of gains in the controller, can be obtained. Experiments on a test system show an excellent performance during startup as well as for variation of cooling capacity by step change of the compressor speed between minimum and maximum. The new controller is also compared to a conventional controller based on a thermostatic expansion valve (TXV) for controlling of the superheat.

2. System description

Refrigeration systems typically use a vapor-compression cycle process to transfer heat from a cold reservoir (e.g. a cold storage room) to a hot reservoir, normally the surroundings. The main idea is to let a refrigerant circulate between two heat exchangers, i.e. an evaporator and a condenser. In the evaporator the refrigerant "absorbs" heat from the cold reservoir by evaporation and "rejects" it in the condenser to the hot reservoir by condensation. In order to establish the required heat transfer, the evaporation temperature (T_e) has to be lower than the temperature in the cold reservoir (T_{cr}) and the condensation temperature (T_c) has to be higher than the temperature in the hot reservoir (normally the surroundings T_a), i.e. $T_e < T_{cr}$ and $T_c > T_a$. The refrigerant has the property (along with other pure fluids and gases) that the saturation temperature (T_{sat}) uniquely depends on the pressure. At low pressure the corresponding saturation temperature is low and vice versa at high pressure. This property is exploited in the refrigeration cycle to obtain a low temperature in the evaporator and a high temperature in the condenser simply by controlling respectively the evaporating pressure (P_e) and the condensing pressure (P_c). Between the evaporator and the condenser is a compressor. The compressor compresses the low pressure refrigerant (P_e) from the outlet of the evaporator to a high pressure (P_c) at the inlet of the condenser, hereby circulating the refrigerant between the evaporator and the condenser. To uphold the pressure difference ($P_c > P_e$) an expansion valve is installed at the outlet of the condenser. The expansion valve is basically an adjustable nozzle that helps upholding a pressure difference.

The test system fig. 1 is a simple refrigeration system with water circulating through the evaporator. The evaporator is a plate heat exchanger, i.e. an evaporator type with a low internal volume. The heat load on the system is maintained by an electrical water heater with an adjustable power supply for the heating element. The compressor, the evaporator fan and the condenser pump are equipped with variable speed drives so that the rotational speed can be adjusted continuously. The system is furthermore equipped with an electronic expansion valve that enables a continuous variable opening degree. The system has temperature and pressure sensors on each side of the components in the refrigeration cycle. Mass flow meters measure the mass flow rates of refrigerant in the refrigeration cycle and water on the secondary side of the evaporator. Temperature sensors measure the inlet and outlet temperature of the secondary media on respectively the evaporator and the condenser. The applied power to the condenser fan and the compressor is measured. Finally the entire test system is located in a climate controlled room, such that the ambient temperature can be regulated. For data acquisition and control the XPC toolbox for SIMULINK is used.

3. Modeling and verification

3.1. Model overview

A detailed model for an evaporator is based on the conservation equations of mass, momentum and energy on the refrigerant, air and tube wall. This leads to a numerical solution of a set of differential equations discretized into a finite difference form, see [11]. This model gives very detailed information to the control designer comparable to the real system. This means that it is useful for testing controllers, but due to the high complexity not for design of new control principles.

A simpler model may be obtained by using a so called moving boundary model for the time dependent two phase flows and by assuming that spatial variations in pressure are negligible, which means that the momentum equation is no longer necessary. The numerical solution may describe the system quite well and results are shown in [12] and [13]. The moving boundary model is very general and may be fitted to most evaporator types.

By simplifying the moving boundary model further a very simple nonlinear model describing the dominating time "constant" and the nonlinear behavior between input and output is

obtained. The gain and time constant variations as a function of the inputs and disturbances are expressed analytically. Following approximations made are

- fluid flow is one-dimensional
- spatial variations in pressure are negligible
- axial conduction is negligible
- cross sectional area of flow stream is constant
- the heat transfer coefficient from water to wall is small compared to the heat transfer coefficient from wall to boiling refrigerant
- the energy for super heating the gas is negligible compared to the energy for evaporating the refrigerant
- the heat capacity of the wall between water and refrigerant is considered to be negligible.

3.2. Energy and mass balance two phase section

The mass and energy of the two phase section are given by

$$\begin{aligned} M_e(t) &= (\rho_l(1-\gamma_e)+\rho_g\gamma_e)BHl_e(t) \\ U_e(t) &= (\rho_l(1-\gamma_e)h_l+\rho_g\gamma_e h_g)BHl_e(t) \end{aligned} \tag{1}$$

where it is assumed that the work associated with the rate of change of pressure with respect to time is negligible. From (1) the following relation is obtained

$$U_e - h_g M_e = -\rho_l(1-\gamma_e)(h_g-h_l)BHl_e \tag{2}$$

If it is further assumed that void fraction γ_e is constant independent of l_e, and variation of h_g and h_l due to pressure variation is neglected, the following relation is obtained

$$\dot{U}_e - h_g\dot{M}_e = -\rho_l(1-\gamma_e)(h_g-h_l)BH\frac{dl_e}{dt} \tag{3}$$

The mass and energy balance is given by

$$\begin{aligned} \dot{M}_e &= \dot{m}_e - \dot{m}_{comp} \\ \dot{U}_e &= h_i\dot{m}_e - h_g\dot{m}_{comp} + \alpha_1 Bl_e(T_w - T_e) \end{aligned} \tag{4}$$

Combining (3) and (4) then gives

$$\rho_l(1-\gamma_e)(h_g-h_l)BH\frac{dl_e}{dt} = (h_g-h_i)\dot{m}_e - \alpha_1 Bl_e(T_w-T_e) \tag{5}$$

The first term on the right side corresponds to the energy difference between the refrigerant leaving and entering the two phase section of the evaporator. The second term is the rate of the heat transfer from water to refrigerant. The left side describes the change of energy of the two phase section. From refrigerant data [14] we have

$$\begin{aligned} h_g &= HDewP(P_e) \\ h_i &= HBubP(P_c) \\ h_l &= HBubP(P_e) \\ T_e &= TDewP(P_e) \\ \rho_g^{-1} &= VDewP(P_e) \\ \rho_l^{-1} &= VBubP(P_e) \end{aligned} \tag{6}$$

Insertion of (1) in (4) then gives

$$\frac{d(\rho_l(1-\gamma_e)+\rho_g\gamma_e)BHl_e}{dP_e}\frac{dP_e}{dt} = \dot{m}_e - \dot{m}_{comp} \tag{7}$$

Assuming the liquid to be incompressible (7) becomes

$$BHl_e\kappa\frac{dP_e}{dt} = \dot{m}_e - \dot{m}_{comp} \tag{8}$$

with $\kappa = \frac{d\rho_g}{dP_e}$.

3.3. Superheat section

If the axial conduction is negligible and the heat capacity of the water $c_w\dot{m}_{water} >> c_{p,e}\dot{m}_e$ the superheat T_{SH} becomes

$$T_{SH} = (T_w - T_e)\left[1 - \exp\left\{-\frac{\alpha_1 B(L_e - l_e))}{c_{p,e}\dot{m}_e}\right\}\right] \tag{9}$$

3.4. Compressor

The piston compressor model is developed from factory given data as

$$\dot{m}_{comp} = \alpha_c P_e f_{comp} \tag{10}$$

where α_c is a function of P_e and P_c. Assuming $P_c = P_{c,ref}$ due to control of the condenser fan the variation of α_c is only caused by variation of P_e. In the working area for the system this variation is less than 5% and α_c is considered as a constant. Equ. (10) in (8) then gives

$$\frac{BHl_e\kappa}{\alpha_c f_{comp}}\frac{dP_e}{dt} = -P_e + \frac{\dot{m}_e}{\alpha_c f_{comp}} \tag{11}$$

3.5. Combined model

$$\begin{aligned} T_e &= TDewP(P_e) \\ c_1\dot{x}_e &= (h_g-h_i)\dot{m}_e - c_0(T_w-T_e)x_e \\ c_2\frac{f_{\min}}{f_{comp}}\dot{P}_e &= -P_e + \frac{\dot{m}_e}{\alpha_c f_{comp}} \\ T_{SH} &= (T_w-T_e)\left[1-\exp\left\{-\frac{1-x_e}{x_\delta}\right\}\right] \end{aligned} \tag{12}$$

with:

a) $c_1 = \rho_l(1-\gamma_e)(h_g-h_l)BH$
b) $c_2 = BHl_e\kappa/(\alpha_c f_{\min})$
b) $c_0 = \alpha_1 BL_e$
c) $x_\delta = c_{p,e}\dot{m}_e/(\alpha_1 BL_e)$
d) $x_e = l_e/L_e$

3.6. Control input and measurement

The control inputs are f_{comp} and $\dot{m}_e$ and the measured values are T_{SH}, P_e and T_w. From these measurements the relative length x_e of the two phase section is obtained by

$$x_{e,meass} = 1 - x_\delta \log\frac{T_w - T_e}{T_w - T_e - T_{SH}} \tag{13}$$

3.7. Model verification

The model parameters to be estimated are (c_1, c_2) and $\theta = (\alpha_c, x_\delta, c_0)$. A series of experiments giving large signal excitation of the system for different working conditions are performed. Simulation using the model (12) with the same input $(\dot{m}_v, f_{comp,ref})$ as used in the experiment then gives the output (P_e, T_{SH}). The constants c_1 and c_2 are first found by visual fitting of simulated and measured values of the output. Using these values for all experiments θ may now be determined by minimizing the performance function

$$J(\theta) = \frac{1}{t_2 - t_1}\int_{t_1}^{t_2}\{K_0(P_e - P_{e,meass})^2 + (T_{SH} - T_{SH,meass})^2\}dt \tag{14}$$

The parameter K_0 determines the weight between squared values of the variation of $(P_e - P_{e,meass})$ and $(T_{SH} - T_{SH,meass})$. A value $K_0 >> 1$ gives a value of α_c resulting in the best fit to the pressure equation, but because the model only is an approximation the influence of the other parameters are hidden in noise. If $K_0 << 1$ the opposite is the case. A reasonable weight between variation of P_e and T_{SH} with respect to model errors seems from many experiments with different K_0 to be the value $K_0 = 50$. The result is shown in table 1

Simulated and measured values for experiment 2 and 4 are shown in fig. (3) and (4). It is seen that the model gives a good description of the dominating dynamics of the system when optimized values are used. Fig. (5) shows the simulated output using the estimated mean values. The dynamics are again well described but DC values are badly modeled. This means that the DC value problem needs a special treatment.

4. Control objectives and challenges

The main focus of this paper is to derive a new control scheme that improves the control performance and the energy efficiency compared to existing control schemes. This is mainly obtained by utilizing a generic model based control. A further advantage, by utilizing simple and generic models is that the scalability of the controllers are maintained. This is an important aspect for mass produced applications like residential air conditioning systems because it enables the control scheme to work on a diversity of system compositions and sizes, with only minor changes.
Being more specific following objectives should be fulfilled by the control:

- Maintain a constant low superheat
- Maintain stable operation under varying operational conditions
- Ability to respond fast to changes in the requested cooling power
- Fast settling time after startup
- Ability to suppress disturbances and follow load variations

The main control challenges in the systems are as previously described the cross couplings and the nonlinearities. Furthermore saturations of the actuators i.e. compressor and valves also complicate the control design. If a variable speed drive for the compressor is used the compressor capacity can continuously be operated between a maximal and a minimal speed. At low speed the lubrication of the compressor stops working, hence limiting the minimally allowable speed the compressor can be operated at. This causes a discontinuity in the lower end of the operating range of the compressor capacity complicating the control design, for exemplification see [15].

5. New control methods

The steady state value of the pressure given by the model

$$c_2\frac{f_{min}}{f_{comp}}\dot{P}_e = -P_e + \frac{\dot{m}_e}{\alpha_c f_{comp}} \tag{15}$$

is proportional to $\dot{m}_e/\alpha_c$. In the model verification section the uncertainty of α_c was shown. The refrigerant flow $\dot{m}_e$ was measured, but in a practical control scheme an estimate of $\dot{m}_e$ has to be used. This means that the gain $\dot{m}_e/\alpha_c$ may have an error up to 30% of the best guess. Because the measured pressure P_e is of good quality a way to overcome this problem is to control the pressure by an PI-controller. The controller

$$\begin{aligned} u = &\quad \frac{\alpha_c}{\tau_0\dot{m}_e}\frac{1 + c_2\frac{f_{\min}}{f_{comp}}p}{p}(P_{e,ref} - P_e) \\ f_{comp} = &\quad \frac{1}{u} \text{ for } u_{\min} < u < u_{\max} \end{aligned} \tag{16}$$

with $u_{\min} > 0$ gives the closed loop for the pressure

$$\tau_0\dot{P}_e = -P_e + P_{e,ref} \tag{17}$$

The gain of the PI-controller (16) is given by

$$c_2\frac{f_{\min}\alpha_c}{f_{comp}\tau_0\dot{m}_e}$$

where τ_0 is the specified closed loop time constant. The gain is seen to be scheduled with the compressor frequency and refrigerant mass flow. If the mass flow is not measured an estimate based on (10) may be used.

The resulting cascaded structure shown in fig. (6) then gives the following model for the relative filling x_e and the superheat temperature

$$\begin{aligned} T_e &= TDewP(P_e) && \text{(a)} \\ c_1\dot{x}_e &= (h_g - h_i)\dot{m}_e - c_0(T_w - T_e)x_e && \text{(b)} \\ \tau_0\dot{P}_e &= -P_e + P_{e,ref} && \text{(c)} \\ T_{SH} &= (T_w - T_e)\left[1 - \exp\left\{-\tfrac{1-x_e}{x_\delta}\right\}\right] && \text{(d)} \end{aligned} \tag{18}$$

The variation in the gain $\dot{m}_e/\alpha_c$ in (15) then only influence the time constant τ_0 in (18.c). The output nonlinearity (18.d) is compensated for by using the inverse nonlinearity in the measurement of x_e (13) The multiplication of the two states x_e and

Table 1: Experiments for model verification

	Experiment		c_1	c_2	α_c	x_δ	c_0	J
1.	$f_{comp} = 40$	and $0.020 < \dot{m}_e < 0.024$	3e5	10	$1.7757e-4$	0.1604	242.6	1.4373
2.	$f_{comp} = 50$	and $0.026 < \dot{m}_e < 0.030$	3e5	10	$1.8682e-4$	0.1310	274.5	1.2464
3.	$f_{comp} = 60$	and $0.029 < \dot{m}_e < 0.033$	3e5	10	$1.8015e-4$	0.1957	294.5	3.2409
4.	$\dot{m}_e = 0.022$	and $35 < f_{comp} < 45$	3e5	10	$1.7925e-4$	0.1429	223.7	2.3106
5.	$\dot{m}_e = 0.028$	and $45 < f_{comp} < 55$	3e5	10	$1.8282e-4$	0.1390	265.2	3.5094
6.	random		3e5	10	$1.7765e-4$	0.1650	238.9	1.9463
7.	random		3e5	10	$1.8673e-4$	0.1494	269.6	1.6897
8.	random		3e5	10	$1.7876e-4$	0.1658	276.1	1.1648
	mean values		3e5	10	$1.8122e-4$	0.1562	260.6	

T_e call for a nonlinear design method if the controller has to be be valid in the hole working area.

The reference value for the pressure may be calculated based on the reference of the evaporating temperature T_{ref} by

$$P_{e,ref} = PDewT(T_{ref}) \tag{19}$$

Because the relation between T_e and P_e is nearly linear in a large operating interval (17) is equivalent to

$$\tau_0 \dot{T}_e = -T_e + T_{ref} \tag{20}$$

The following bilinear model for the relative filling x_e and the evaporation temperature T_e may then be used for the controller design

$$\begin{array}{ll} c_1 \dot{x}_e & = (h_g - h_i)\dot{m}_e - c_0 x_e (T_w - T_e) \\ \tau_0 \dot{T}_e & = -T_e + T_{ref} \end{array} \tag{21}$$

In (21) x_e has to be controlled to a value x_e^0 by T_{ref}. If T_e was the control input then for constant x_e^0

$$c_1 p(x_e - x_e^0) = -k_1(x_e - x_e^0) \tag{22}$$

is obtained by the value T_e^0 calculated by (23)

$$c_0 x_e^0 (T_w - T_e^0) = (h_g - h_i)\dot{m}_e + k_1(x_e - x_e^0) \tag{23}$$

The value for the tuning parameter k_1 is found by the Lyapunov analysis.

Insertion of (23) in (21) gives

$$\begin{array}{l} c_1 p(x_e - x_e^0) = \\ -(k_1 + c_0(T_w - T_e))(x_e - x_e^0) + c_0 x_e^0 (T_e - T_e^0) \\ \\ \tau_0 p(T_e - T_e^0) = \\ -(T_e - T_e^0) + T_{ref} - T_e^0 - \tau_0 p T_e^0 \end{array} \tag{24}$$

For $k_2 > 0$ the Lyapunov function candidate

$$P = \tfrac{1}{2} c_1 (x_e - x_e^0)^2 + \tfrac{1}{2}\tau_0 k_2 (T_e - T_e^0)^2 \tag{25}$$

is positive definite and has the time derivative

$$\begin{array}{l} \dot{P} = \\ -(k_1 + c_0(T_w - T_e))(x_e - x_e^0)^2 - k_2(T_e - T_e^0)^2 \\ +(T_e - T_e^0) k_2 (T_{ref} - (1 + \tau_0 p)T_e^0 + \dfrac{c_0 x_e^0}{k_2}(x_e - x_e^0)) \end{array} \tag{26}$$

For a control input T_{ref} given by

$$T_{ref} = (1 + \tau_0 p)T_e^0 - \frac{c_0 x_e^0}{k_2}(x_e - x_e^0) \tag{27}$$

the time derivative of the Lyapunov function becomes

$$\dot{P} = -(k_1 + c_0(T_w - T_e))(x_e - x_e^0)^2 - k_2(T_e - T_e^0)^2 \tag{28}$$

This function is negative definite for positive $k_1 + c_0(T_w - T_e) > 0$ and $k_2 > 0$, leading to a stable closed loop system.

The new backstepping controller

$$\begin{array}{lll} T_e^0 & = T_w - \dfrac{1}{c_0 x_e^0}\left((h_g - h_i)\dot{m}_e + k_1(x_e - x_e^0)\right) & (a) \\ T_{ff} & = (1 + \tau_0 p)T_e^0 & (a) \\ T_{ref} & = T_{ff} + \frac{c_0 x_e^0}{k_2}(x_e^0 - x_e) & (b) \\ P_{e,ref} & = PDewT(T_{ref}) & (b) \\ u & = \frac{\alpha_c}{\tau_0 \dot{m}_e} \frac{1 + c_2 \frac{f_{\min}}{f_{comp}} p}{p}(P_{e,ref} - P_e) & (c) \\ u & = sat(u, u_{\min}, u_{\max}) & (c) \\ f_{comp} & = \frac{1}{u} & (c) \end{array} \tag{29}$$

The structure of the developed backstepping controller (29) is shown in fig. 7 and is tested on a simulation model based on estimated mean value model parameters. The result is shown in fig. 8 for the following controller parameters

$$\begin{array}{l} \tau_0 = 2 \\ k_1 = 0 \\ k_2 = 100 \\ x_e^0 = 0.9 \end{array} \tag{30}$$

It is seen that the variation in x_e caused by the variation in $\dot{m}_e$ is small due to the small time constant τ_0 for the pressure controller. In the controller c_0 is assumed known leading to a steady state $\dot{m}_e$ equal to the reference.

Fig. 9 shows the simulated output if c_0 is changed during the simulation. The figure shows the need for an adaptation of the c_0 value.

6. Adaptive backstepping control

Adaptation of c_0 is based on the following modification of the Lyapunov function (25)

$$P = \tfrac{1}{2} c_1 (x_e - x_e^0)^2 + \tfrac{1}{2}\tau_0 k_2 (T_e - T_e^0)^2 + \frac{1}{\gamma}(c_0 - \hat{c}_0)^2 \tag{31}$$

where $\hat{c}_0$ is the estimate of c_0. P is positive definite for $k_2 > 0$ and $\gamma > 0$. Defining T_e^0 by

$$\hat{c}_0 x_e^0 (T_w - T_e^0) = (h_g - h_i)\dot{m}_e + k_1(x_e - x_e^0) \tag{32}$$

leads for constant x_e^0 to the equation

$$\begin{aligned} &c_1 p(x_e - x_e^0) = \\ &-(k_1 + \hat{c}_0(T_w - T_e))(x_e - x_e^0) + \hat{c}_0 x_e^0 (T_e - T_e^0) \\ &-(c_0 - \hat{c}_0) x_e (T_w - T_e) \end{aligned} \tag{33}$$

$$\begin{aligned} &\tau_0 p(T_e - T_e^0) = \\ &-(T_e - T_e^0) + T_{ref} - T_e^0 - \tau_0 p T_e^0 \end{aligned}$$

The time derivative of P then becomes

$$\begin{aligned} &\dot{P} = \\ &-(k_1 + \hat{c}_0(T_w - T_e))(x_e - x_e^0)^2 - k_2(T_e - T_e^0)^2 \\ &+(T_e - T_e^0) k_2 (T_{ref} - (1 + \tau_0 p) T_e^0 + \frac{\hat{c}_0 x_e^0}{k_2}(x_e - x_e^0)) \\ &-(c_0 - \hat{c}_0)\left((x_e - x_e^0) x_e (T_w - T_e) + \tfrac{1}{\gamma}(p\hat{c}_0)\right) \end{aligned} \tag{34}$$

For a control input T_{ref} given by

$$T_{ref} = (1 + \tau_0 p) T_e^0 - \frac{\hat{c}_0 x_e^0}{k_2}(x_e - x_e^0) \tag{35}$$

and the adaptation law

$$(p\hat{c}_0) = -\gamma(x_e - x_e^0) x_e (T_w - T_e) \tag{36}$$

the time derivative of the Lyapunov function becomes

$$\dot{P} = -(k_1 + \hat{c}_0(T_w - T_e))(x_e - x_e^0)^2 - k_2(T_e - T_e^0)^2 \tag{37}$$

This function is negative definite for positive

$$k_1 + \hat{c}_0(T_w - T_e) > 0 \text{ and } k_2 > 0 \tag{38}$$

leading to a stable closed loop system.

The adaptive backstepping controller

$$\begin{aligned} T_e^0 &= T_w - \frac{1}{\hat{c}_0 x_e^0}\left((h_g - h_i)\dot{m}_e + k_1(x_e - x_e^0)\right) \\ T_{ff} &= (1 + \tau_0 p) T_e^0 \\ T_{ref} &= T_{ff} - \frac{\hat{c}_0 x_e^0}{k_2}(x_e - x_e^0) \\ P_{e,ref} &= PDewT(T_{ref}) \\ u &= \frac{\alpha_c}{\tau_0 \dot{m}_e} \frac{1 + c_2 \frac{f_{\min}}{f_{comp}} p}{p}(P_{e,ref} - P_e) \\ u &= sat(u, u_{\min}, u_{\max}) \\ f_{comp} &= \frac{1}{u} \\ \frac{d\hat{c}_0}{dt} &= -\gamma(x_e - x_e^0) x_e (T_w - T_e) \end{aligned} \tag{39}$$

The adaptive controller (39) is identical to (29) with the extension of the update law for $\hat{c}_0$ and the constant c_0 in (29) has been replaced with the estimate $\hat{c}_0$ in (39). The simulation shown in Fig. 9 where c_0 is changed during the simulation is repeated with the adaptive backstepping controller given in equ. (39). The result is shown in fig. 10 where estimation of $\hat{c}_0$ gives correct steady state value of x_e.

Stability

The stability is proven by the Lyapunov analysis, except for the situation where u saturates. Because the system is open loop stable then saturation of u will not cause instability and implementation of the PI-controller with anti integrator windup [16] gives proper operation as seen in the startup experiment in fig. 15.

7. Experiments

Figure 11 shows the controller for constant $x_{e,ref}$ and variation of the cooling capacity by a step up of $\dot{Q}_e = (h_g - h_i)\dot{m}_e$. The controller keeps T_{SH} at a nearly constant value independent of the cooling. Figure 12 shows a step down of $\dot{Q}_e = (h_g - h_i)\dot{m}_e$ and again tracking time for $\hat{c}$ gives the deviation from the reference of T_{SH}.

Figure 13 shows the estimated parameter c_0 for a step in $\dot{Q}_e$ at a nearly constant temperature $T_{w,in}$ of the water inlet. The tracking time constant shown is seen to explain the time for the deviation of T_{SH} from the reference in fig. 11 and 12.

Figure 14 shows the estimated parameter c_0 for a constant $\dot{Q}_e$ and variation of the water inlet temperature $T_{w,in}$.

Figure 15 shows a startup of the system. The settling time is mainly due to the response of the condensator pressure controller which for the evaporator controller is seen as a disturbance.

Fig. 16 shows the result from the conventional control system shown in Fig. 1. The superheat is controlled by the opening of the thermostatic expansion valve (TXV) and the cooling capacity by the compressor speed. This figure should be compared to Fig. 11 and Fig. 12. The coupling between superheat and cooling capacity is seen to be considerably larger than for the new controller. This means that tuning of the controller for cooling of the system influences the total performance considerably [17]. A common way to obtain a proper performance is to tune the cooling controller to be slow compared to the superheat controller.

7.1. Energy efficiency

Due to the limits of the compressor speed continuous superheat control is only possible for

$$f_{\min} \le f_{comp} \le f_{\max} \tag{40}$$

If the refrigerant flow $\dot{m}_e = \dot{m}_{e,\max}$ gives a compressor speed $f_{comp} = f_{\max}$ then $\dot{m}_e > \dot{m}_{e,\max}$ gives a reduced superheat temperature and may lead to liquid refrigerant into the compressor. This means that the upper limit for the cooling capacity should be set to $\dot{Q}_{e,\max} = (h_g - h_i)\dot{m}_{e,\max}$.

If the refrigerant flow $\dot{m}_e = \dot{m}_{e,\min}$ gives a compressor speed $f_{comp} = f_{\min}$ then $\dot{m}_e < \dot{m}_{e,\min}$ gives an increased superheat. This is acceptable seen from a control point of view, but the energy efficiency is decreased. This means that continuous control of the cooling $\dot{Q}_e = (h_g - h_i)\dot{m}_e$ is possible for all $\dot{Q}_e < \dot{Q}_{e,\max}$.

For $\dot{Q}_e < \dot{Q}_{e,\min} = (h_g - h_i)\dot{m}_{e,\min}$ the superheat controller is saturated leading to an increased superheat temperature.

Efficiency κ_e is based on a steady state experiment by calculating

$$\begin{aligned} \dot{Q}_{e,0}(k) &= \frac{1}{T_0}\int_{(k-1)T_0}^{kT_0} \dot{Q}_e(\tau)d\tau \\ \dot{Q}_{comp,0}(k) &= \frac{1}{T_0}\int_{(k-1)T_0}^{kT_0} \dot{Q}_{comp}(\tau)d\tau \\ \kappa_e(k) &= \dot{Q}_{e,0}(k)/\dot{Q}_{comp,0}(k) \end{aligned} \tag{41}$$

A way to overcome the problem with decreased efficiency for $\dot{Q}_e < \dot{Q}_{e,\min}$ is to periodically (T_0) start and stop the refrigerant flow/compressor and then control the mean value of the refrigerant flow by the duty cycle. If the system to be cooled down has a dominating time constant $T_{system} \gg T_0$, then the variation in temperature due to the start/stop is small and the cooling controller may act as a discrete time controller with sampling time T_0, and the duty cycle as control input. The two situations are referred to as *continuous control* and *PWM control* in the following.

A comparison between continuous control and PWM control for the new controller is shown in Fig. 17. It is seen that PWM control is more energy efficient for small cooling capacities. The reason for that is that if the continuous controller gives a refrigerant flow $\dot{m}_e < \dot{m}_{e,\min}$ the compressor speed saturates at $f_{comp} = f_{\min}$ resulting in an increased superheat. This is acceptable seen from a control point of view, but the energy efficiency is decreased due to the reduced filling of the evaporator

Fig. 18 shows the same comparison between continuous control and PWM control for a conventional system controlled by a thermostatic expansion valve. In this system it is not possible to make continuous control for $\dot{Q}_e < \dot{Q}_{e,\min}$. Otherwise the performance is very like the performance of the backstepping controller shown in Fig. 17.

8. Conclusion

A new control strategy where the superheat temperature is controlled by the compressor and the cooling capacity by the refrigerant mass flow is compared to a conventional control strategy based on a thermostatic expansion valve for control of the superheat. A low order model for the highly nonlinear system with compressor speed as input to the superheat output is derived. This model is used in a nonlinear backstepping design method. The developed method gives a superheat control which is nearly independent of the cooling capacity. The stability of the proposed method is validated theoretically by the Lyapunov analysis and experimental results show the stable performance of the system for a wide range of operating points. Compared to other methods no gain scheduling of the superheat controller is necessary to cover a large region of operation.

The experiments and simulations show that the backstepping controller maintain continuous control at all requested cooling capacities, thus enabling precise temperature control. The price of having continuous control at low capacities is however a reduced efficiency compared to PWM control. Comparison of the backstepping control with a TXV showed that the backstepping control can provide similar performance to the TXV. The advantage of the backstepping control is however that it offers a higher flexibility in the system control than the TXV and it provides the possibility to switch to PWM control at low capacities thus optimizing the overall efficiency at all capacities.

References

[1] Larsen,L.F.S., and Thybo,C.: 'Potential energy savings in refrigeration systems using optimal set-points'. Conference on Control Applications, Taiwan, 2004

[2] Larsen,L.F.S., and Thybo,C., and Stoustrup,J., and Rasmussen,H.: 'A method for online steady state energy minimization, with application to refrigeration systems'. Conference on Decision and Control, Bahamas, 2004

[3] Parkum,J., and Wagner,C.: 'Identification and control of a dry-expansion evaporator'. 10th IFAC symposium on system identification, 1994

[4] Larsen,L.F.S.: 'Model Based Control of Refrigeration Systems'. Ph.D. Thesis ISBN 87-90664-29-9, Aalborg University / Danfoss A/S, 2005

[5] Changquin T., and Chunpeng D., and Xinjiang Y., and Xianting L.: 'Instability of automotive air conditioning system with a variable displacement compressor. Part 1. Experimental investigation'. International Journal of Refrigeration, no28, 2005.

[6] Xiang-Dong,H., and Liu,S., and Assada,H.H., and Itoh,H.: 'Multivariable control of vapor compression system'. VAC&R Research, 1998

[7] Zhao,L., and Zaheeruddin,M.: 'Dynamic simulation and analysis of water chiller refrigeration system'. Applied Thermal Engineering, 2005, **25**, 2258–2271.

[8] Xiang-Dong,H., and Asada,H.H.: 'A new feedback linearization approach to advanced control of multi-unit HVAC systems'. American Control Conference, 2003

[9] Rasmussen, H.: 'Nonlinear Superheat Control of a Refrigeration Plant'. Conference on Control Applications, San Antonio, USA, 2008

[10] Rasmussen, H.: 'Nonlinear Superheat Control of a Refrigeration Plant using Backstepping'. IECON'08, Orlando, Florida, USA, Nov.2008

[11] Jia,X., and Tso,C.P., and Jolly,P., and Wong,Y.W.: 'Distributed steady and dynamic modeling of dry-expansion evaporators'. Int. Journal of Refrigeration, 1999, **22**, 126–136.

[12] Grald,E.W., and MacArthur,J.W.: 'Moving boundary formulation for modeling time-dependent two-phase flows'. Int. J. heat and Fluid Flow, 1992, **13**, 266–272.

[13] He, X.D., and Asada,H.H., and Liu,S., and Itoh,H.: 'Multivariable control of vapor compression systems'. HVAC&R Research, 1998, **4**, 205–230.

[14] Skovrup,M.J.: 'Thermodynamic and Thermophysical Properties of Refrigerants'. Ver. 3.00, Technical University of Denmark, 2000

[15] Thybo,H., and Larsen,L.F.S., and Stoustrup,J., and Rasmussen,H.: 'Control of systems with costs related to switching applications to air-condition systems, CCA, Saint Petersburg, Russia, 2009

[16] Aaström, K.J., and Wittenmark,B.: 'Adaptive Control - Second Edition', Addison-Wesley, 1995.

[17] Broerson,P.M.T., and Jagt,M.T.G. van der: Hunting of Evaporators Controlled by a Thermostatic Expansion Valve. ASME J. Dynamic Systems, Measurements, and Control, 1980, **102**, 130–135.

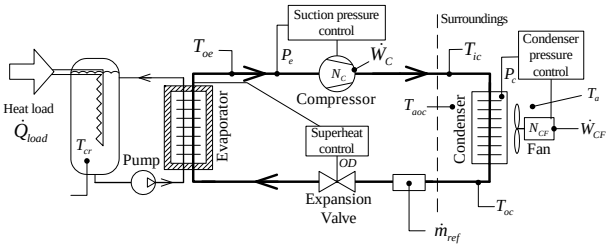

Figure 1: Layout of the test refrigeration system including conventional control loops.

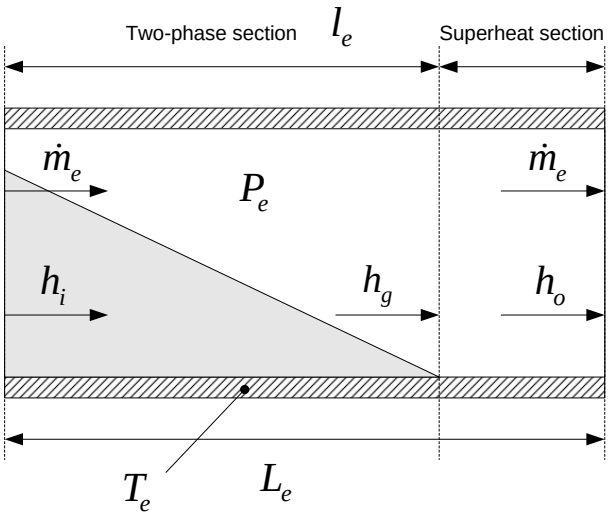

Figure 2: Schematic drawing of the evaporator

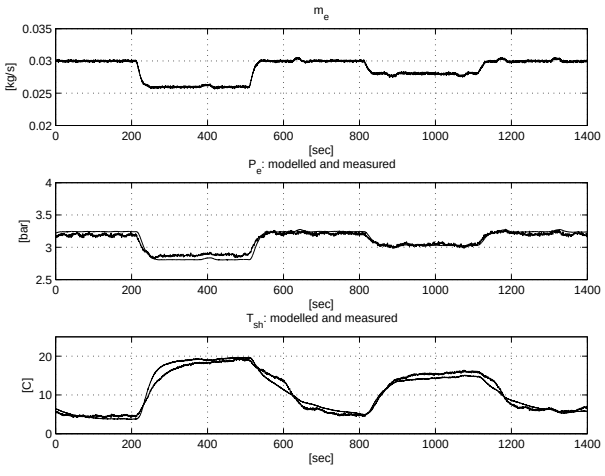

Figure 3: Modeled and measured P_e and T_{sh} for variation of input $\dot{m}_e$

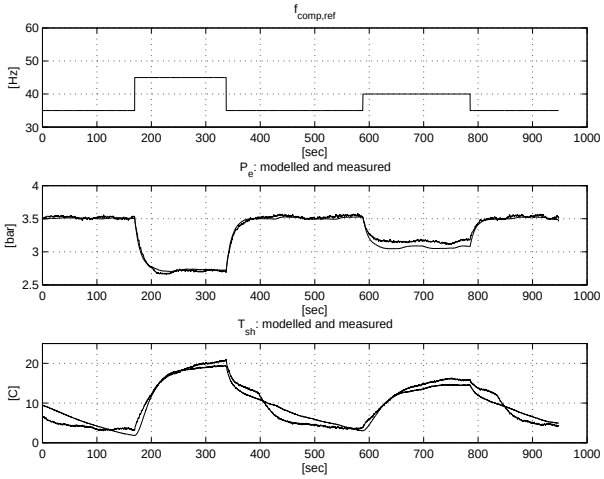

Figure 4: Modeled and measured P_e and T_{sh} for variation of input f_{comp}

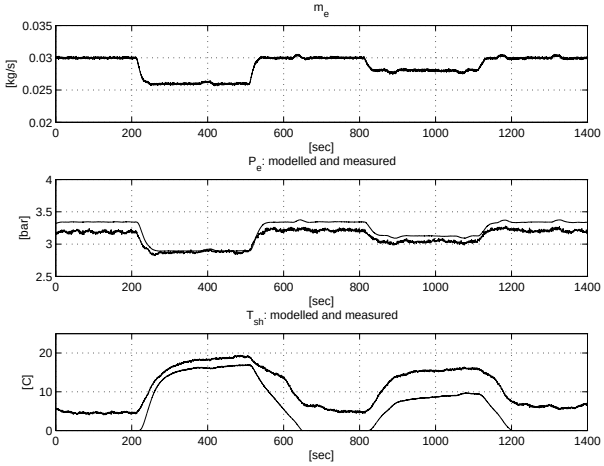

Figure 5: Modeled and measured P_e and T_{sh} for variation of input $\dot{m}_e$ using estimated mean values

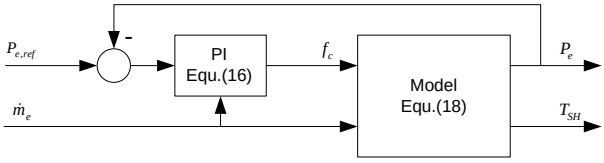

Figure 6: Model with PI control of input f_c.

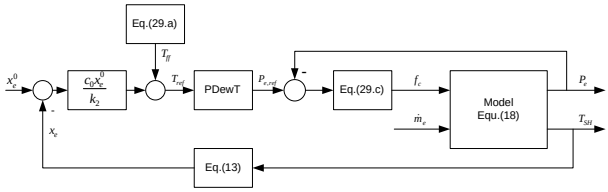

Figure 7: Backstepping controller structure

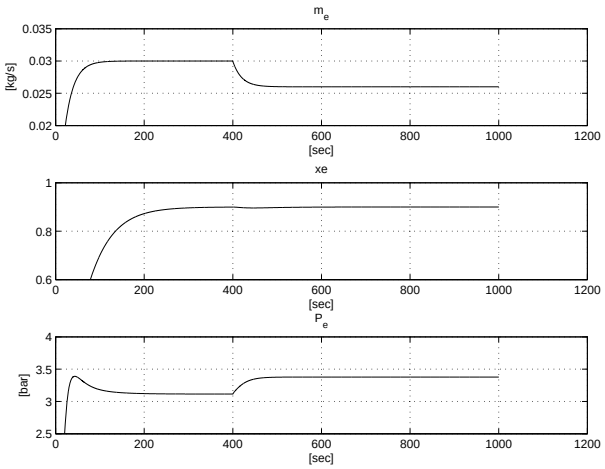

Figure 8: simulated x_e and P_e for variation of input $\dot{m}_e$ using the backstepping controller for known parameters

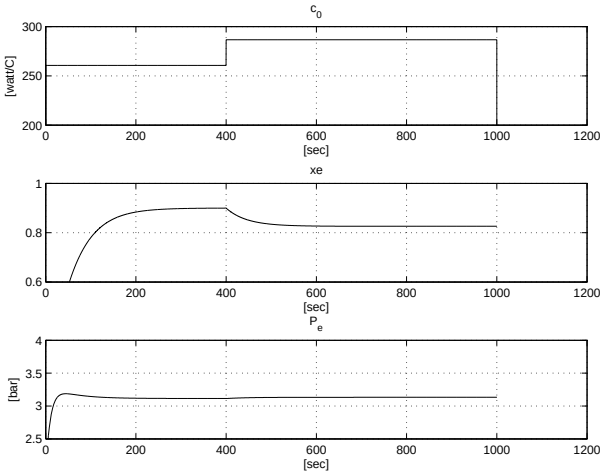

Figure 9: simulated x_e and P_e for variation of c_0 using the backstepping controller for constant c_0 equal to the value before the change.

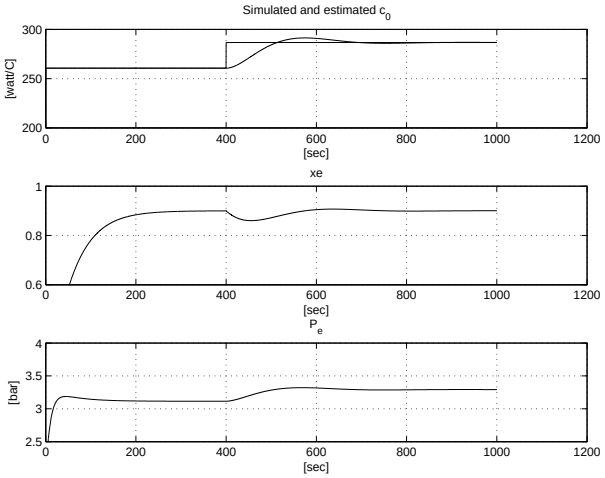

Figure 10: simulated x_e and P_e for variation of c_0 using the adaptive backstepping controller.

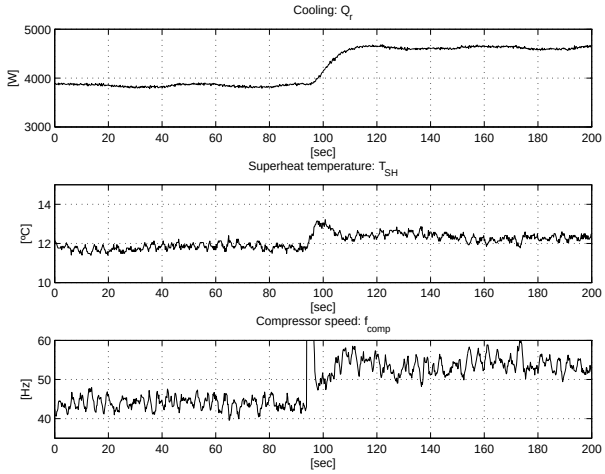

Figure 11: Control of superheat due to disturbance caused by a step up of the cooling.

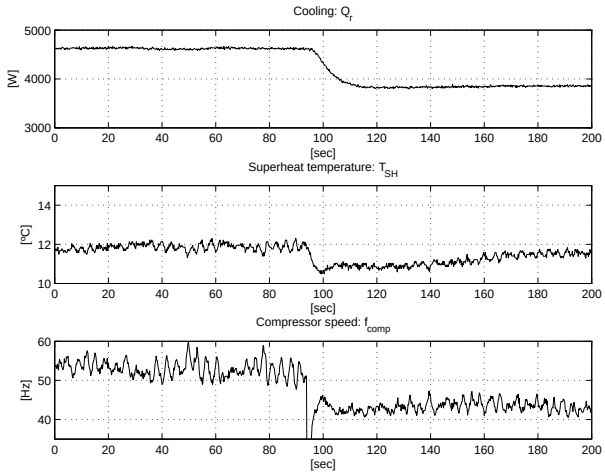

Figure 12: Control of superheat due to disturbance caused by a step down of the cooling.

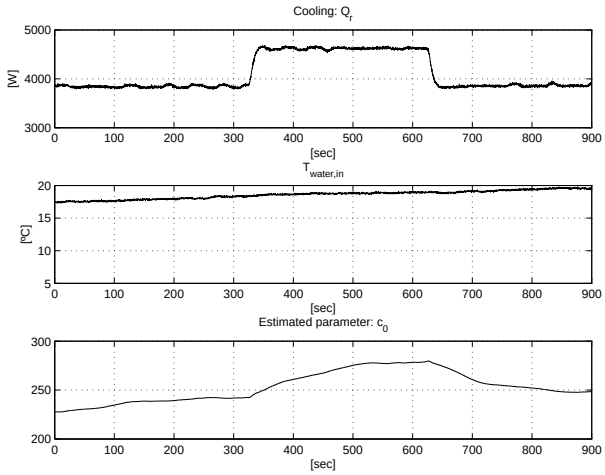

Figure 13: Estimated $\hat{c}$ for variation in cooling capacity Q_r and constant temperature of the water inlet $T_{w,in}$

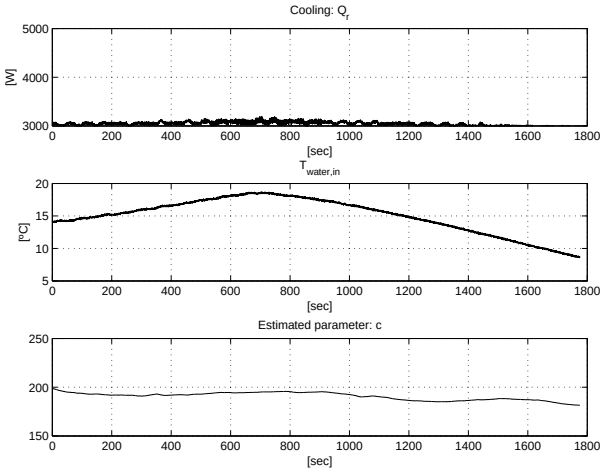

Figure 14: Estimated $\hat{c}$ for constant cooling capacity Q_r and variation of the temperature of the water inlet $T_{w,in}$

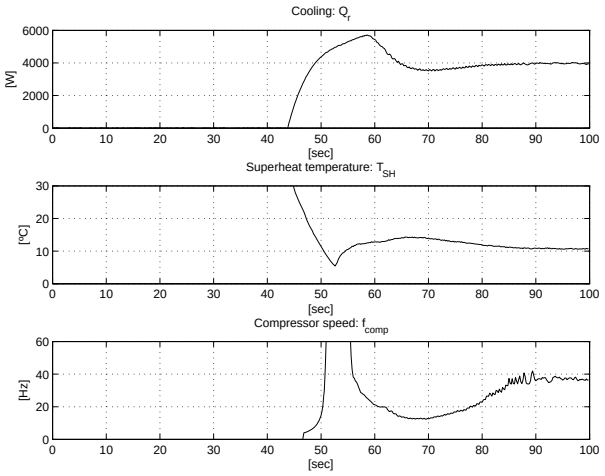

Figure 15: Startup of the system.

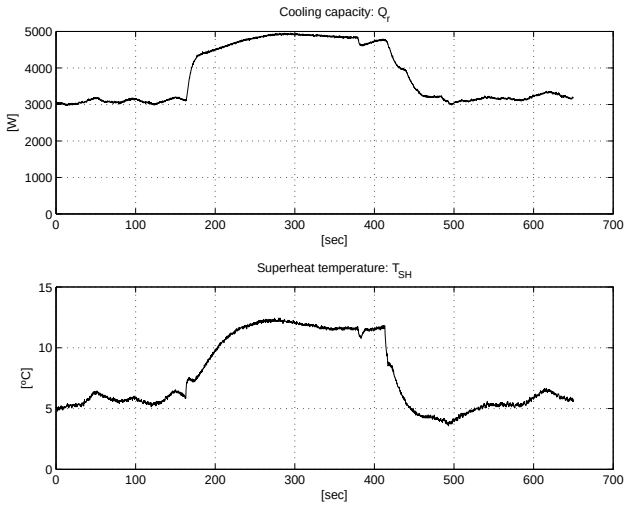

Figure 16: Conventional control by a thermostatic valve.

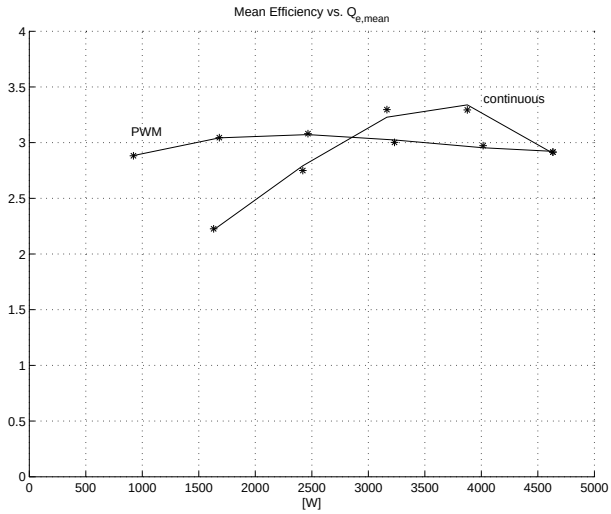

Figure 17: New controller: Mean value the efficiency as a function of mean value of the cooling.

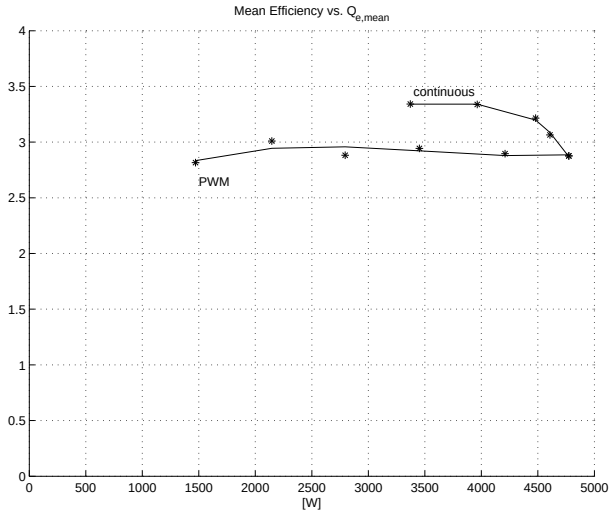

Figure 18: TXV controller: Mean value the efficiency as a function of mean value of the cooling for the conventional controller.